

## Magnetic vortex formation and gyrotropic mode in nanodisks

D. Toscano, S. A. Leonel, R. A. Dias, P. Z. Coura, J. C. S. Rocha, and B. V. Costa

Citation: *Journal of Applied Physics* **109**, 014301 (2011); doi: 10.1063/1.3526970

View online: <http://dx.doi.org/10.1063/1.3526970>

View Table of Contents: <http://scitation.aip.org/content/aip/journal/jap/109/1?ver=pdfcov>

Published by the [AIP Publishing](#)

---

### Articles you may be interested in

[Modelling of micro-Hall sensors for magnetization imaging](#)

*J. Appl. Phys.* **115**, 17E506 (2014); 10.1063/1.4862090

[Radial-spin-wave-mode-assisted vortex-core magnetization reversals](#)

*Appl. Phys. Lett.* **100**, 172413 (2012); 10.1063/1.4705690

[Tailoring the vortex core in confined magnetic nanostructures](#)

*J. Appl. Phys.* **111**, 07D116 (2012); 10.1063/1.3675989

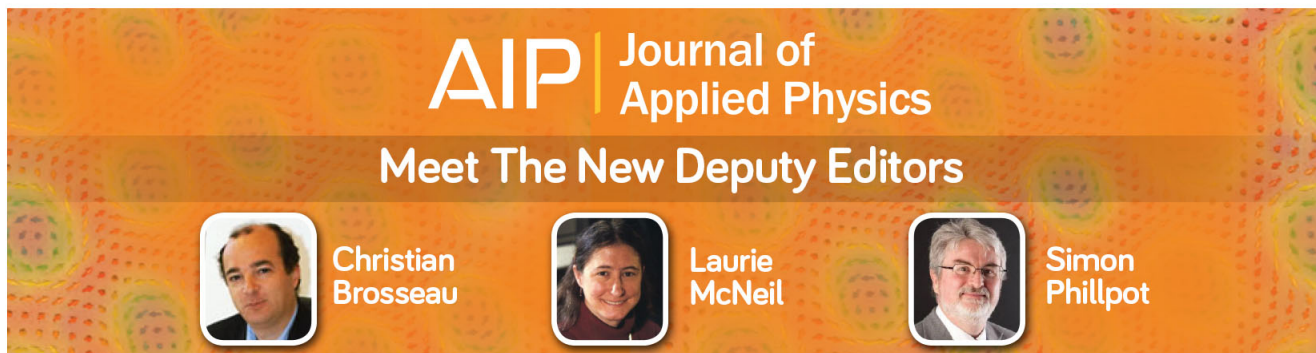
[Magnetic interaction effect on the critical switching current in vortex arrays](#)

*J. Appl. Phys.* **109**, 103906 (2011); 10.1063/1.3590333

[Effect of the classical ampere field in micromagnetic computations of spin polarized current-driven magnetization processes](#)




*J. Appl. Phys.* **97**, 10C713 (2005); 10.1063/1.1853291

---



**AIP** | Journal of Applied Physics

## Meet The New Deputy Editors

	<b>Christian Brosseau</b>		<b>Laurie McNeil</b>		<b>Simon Phillpot</b>
---	---------------------------	---	----------------------	---	-----------------------

## Magnetic vortex formation and gyrotropic mode in nanodisks

D. Toscano,<sup>1,a)</sup> S. A. Leonel,<sup>1,b)</sup> R. A. Dias,<sup>1,c)</sup> P. Z. Coura,<sup>1,d)</sup> J. C. S. Rocha,<sup>2,e)</sup> and B. V. Costa<sup>2,f)</sup>

<sup>1</sup>*Departamento de Física, Laboratório de Simulação Computacional, ICE, UFJF, 36036-330 Juiz de Fora, MG, Brazil*

<sup>2</sup>*Departamento de Física, Laboratório de Simulação, ICEX, UFMG, 30123-970 Belo Horizonte, MG, Brazil*

(Received 15 July 2010; accepted 12 November 2010; published online 3 January 2011)

The superparamagnetic limit imposes a restriction on how far the miniaturization of electronic devices can reach. Recently it was shown that magnetic thin films with nanoscale dimensions can exhibit a vortex as its ground state. The vortex can lower its energy by developing an out-of-plane magnetization perpendicular to the plane of the film, the  $z$  direction, which can be “up” or “down.” Because the vortex structure is very stable this twofold degeneracy opens up the possibility of using a magnetic nanodisk as a bit of memory in electronic devices. The manipulation of the vortex and a way to control the core magnetization is a subject of paramount importance. Recent results have suggested that the polarity of a vortex core could be switched by applying a pulsed magnetic field in the plane of the disk. Another important effect induced by an external magnetic field due to the component out-of-plane in vortex-core is the gyrotropic mode. The gyrotropic mode is the elliptical movement around the disk center executed by the vortex-core under the influence of a magnetic field. In the present work we used numerical simulations to study the ground state as well as the dynamical behavior of magnetic vortices in thin nanodisks. We have considered a model where the magnetic moments interact through exchange  $(-J\vec{S}_i \cdot \vec{S}_j)$  and dipolar potentials  $\{D\Sigma[\vec{S}_i \cdot \vec{S}_j - 3(\vec{S}_i \cdot \hat{r}_{ij}) \times (\vec{S}_j \cdot \hat{r}_{ij})]/r_{ij}^3\}$ . We have investigated the conditions for the formation of the vortex-core with and without an out-of-plane magnetization as a function of the strength of the dipole interaction  $D$  and of the size and thickness of the magnetic nanodisk. Our results were consistent with the existence of two vortex phases separated by a crossover line  $[(D_c - D)^\alpha]$ . We have observed that  $D_c$  does not depend on the radius of nanodisk but depends on its thickness. The exponent  $\alpha$  was found to be  $\alpha \approx 0.55(2)$ . The gyrotropic motion is studied by applying an external magnetic field parallel to the plane of the magnetic nanodisk. Our results show that there is a minimum value for the modulus of the out-of-plane vortex-core magnetization, from which we can excite the gyrotropic mode. This minimum value depends on the thickness of the nanodisk. This result suggest that an experimental way to improve the stability of the process of switching may be through the thickness control. We also observed that the gyrotropic mode frequency increases with the aspect ratio, which is in qualitatively accordance with theoretical and experimental results. Finally, we present theoretical results for Permalloy nanodisks obtained from our model, which are also in good agreement with experimental results. © 2011 American Institute of Physics.

[doi:10.1063/1.3526970]

### I. INTRODUCTION

In the last few years, significant attention has been dedicated to the search for a substitute for magnetic storage devices used so far.<sup>1–11</sup> The reason for that is that miniaturization has a natural limit imposed by thermal fluctuations which determines how long the magnetization of a magnetic structure survives.<sup>12</sup> That is the well known superparamagnetic limit. Developments in nanostructured magnetic materials has shown that the development of a vortex in quasi-two-dimensional (2D) nanomagnets can help to overcome the superparamagnetic limit. It was observed that the ground

state of a small ferromagnetic pellet may have a vortex like structure. By a vortex we mean a special configuration of magnetic moments similar to the stream lines of a circulating flow in a fluid. The magnetic moments precess by  $\pm 2\pi$  on a closed path around the vortex center as shown schematically in the Fig. 1. The importance of vortices in magnetic systems is known since the early seventies in connection with the Berezinskii–Kosterlitz–Thouless phase transition.<sup>13,14</sup> In a finite system the competition between the magnetostatic energy and the exchange interaction is responsible for the formation of a magnetic vortex in the ground state.<sup>15,16</sup> Surface effects become increasingly important as the particle size decreases.<sup>17</sup> The energy associated with a vortex is proportional to  $\ln R$ , where  $R$  is the vortex size. The logarithmic behavior of the energy prohibits the existence of an odd number of vortices (or antivortices) in a system with free or periodic boundary conditions. For a sufficiently large system all the configurations are equally likely. In a magnetic nano-

<sup>a)</sup>Electronic mail: danilotoscano@yahoo.com.br.

<sup>b)</sup>Electronic mail: sidiney@fisica.ufjf.br.

<sup>c)</sup>Electronic mail: radias@fisica.ufjf.br.

<sup>d)</sup>Electronic mail: pablo@fisica.ufjf.br.

<sup>e)</sup>Electronic mail: jcsrocha@fisica.ufmg.br.

<sup>f)</sup>Electronic mail: bvc@fisica.ufmg.br.

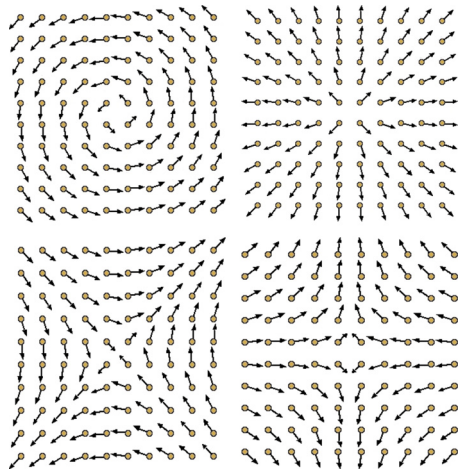


FIG. 1. (Color online) Schematic view of vortices of type *I* and *II* (top) and antivortices (bottom) configurations. In an infinite system all four configurations have the same energy.

disk a magnetic dipole-dipole energy term has to be considered beside exchange and anisotropic terms. The dipole energy competes with the exchange term so that for large enough dipole interaction the continuity of the magnetic field in the boundary of the system imposes the magnetic moments to be tangent to the border of the nanodisk. This kind of boundary condition favors the appearing of an isolated vortex at the center of the system. Although, the vortices and antivortices shown in Fig. 1 have the same bulk energy competition with the border energy clearly favors the appearing of the type *I* vortex.

Due to the singularity at the vortex center the system can lower its energy by developing an out-of-plane magnetization, perpendicular to the plane of the disk, the  $z$  direction which can be “up” or “down” ( $\pm z$ , respectively).<sup>18–22</sup> Due to the out-of-plane component, the simplest effect induced by an external field is the gyrotropic mode, which is a sub gigahertz characteristic excitation of the vortex structure. If the external fields are weak enough, the vortex core behaves like a particle during its motion and its dynamics can be described using a Thiele approach.<sup>23–25</sup> The vortex core polarization (up or down) determines the sense of gyration in trajectory (clockwise or counterclockwise).<sup>26–31</sup> Theoretically we can write a model Hamiltonian for a magnetic nanodisk in a pseudo-spin language as<sup>32</sup>

$$H = -J \sum_{\langle i,j \rangle} \vec{S}_i \cdot \vec{S}_j + D \sum_{i \neq j} \left[ \frac{\vec{S}_i \cdot \vec{S}_j}{r_{ij}^3} - \frac{3(\vec{S}_i \cdot \vec{r}_{ij}) \times (\vec{S}_j \cdot \vec{r}_{ij})}{r_{ij}^5} \right], \quad (1)$$

where  $J$  is the exchange coupling constant,  $\vec{S}_i$  and  $\vec{S}_j$  are spins located in the sites  $i$  and  $j$  satisfying the condition  $|\vec{S}_i| = 1$ ,  $r_{ij}$  is the distance between these sites, and  $D$  is the dipole strength. The sum in the first term is over first neighbors. In the second term the sum runs over the entire lattice. Because the Hamiltonian is invariant under a global operation  $S^z \rightarrow -S^z$  the out-of-plane structure developed at the center of the vortex is degenerated and does not depend on the vortex orientation (clockwise or counterclockwise). These properties opens up the possibility of using a magnetic nano-

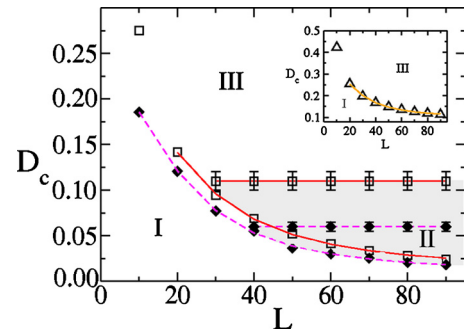


FIG. 2. (Color online) The figure shows the diagram for the vortex formation in three different types of lattices. Squares and diamonds are for the square and the hexagonal lattices, respectively. The inset shows the results for the triangular lattice. Region I and III have a capacitor and a vortex in the ground state, respectively. The shadowed area (region II) represents a region where the most stable configuration has an out-of-plane component at the center of the vortex. The lines separating the capacitor and the vortex states regions are adjusted using the equation  $D_c = D_0 + 1/A(1 + BL^2)$  with the appropriate values of the constants  $D_0$ ,  $A$ , and  $B$ , for each type of lattice. Results from Ref. 34.

disk as a bit element in digital memory devices. The main problem to be surpassed is the effective control of the  $z$  component. The knowledge of the mechanisms behind the appearing of the out-of-plane component of the vortex and how to manipulate it is of paramount importance. Some theoretical modeling suggested that the reversal mechanism is mediated by the creation and annihilation of a vortex anti-vortex pair. A recent experiment using high-resolution time-resolved magnetic x-ray microscopy seems to give support to that mechanism.<sup>33</sup>

In an earlier paper<sup>34</sup> the authors investigated the conditions for the formation of vortices in nanodisks modeled by magnetic moments with dipole–dipole and exchange interactions as in Eq. (1). The effect of varying the lattice size and the strength of the dipole interaction were considered. The results showed that there is a threshold line separating the vortex state from a capacitorlike state (single-domain magnetization). Inside the “vortex phase” it was possible to identify two characteristic regions depending on the dipole–dipole interaction strength  $D$ : an in-plane vortex (in-plane region) and a vortex with an out-of-plane magnetization in its core,  $S_{core}^z$  (out-of-plane region). The results are summarized in Fig. 2.

In the present paper we focus our attention in three main subjects: (1) the conditions for the appearing of a vortex in the ground state as a function of the thickness of the nanodisk; (2) the conditions for the formation of an out-of-plane magnetization at the vortex core as a function of the strength of the dipole interaction; and (3) the behavior of a vortex in the presence of an external magnetic field. The study is carried out by using numerical simulations which will be described in more details in the following. The simulations were performed by considering the dipolar term with and without a cut-off. The results show clearly that the cut-off in the dipolar interaction has to be taken very carefully. We observed that the region where the out-of-plane vortex component appears not depends on the diameter of the nanodisk but the thickness. The increased thickness works as an effective anisotropy inducing larger out-of-plane components, as

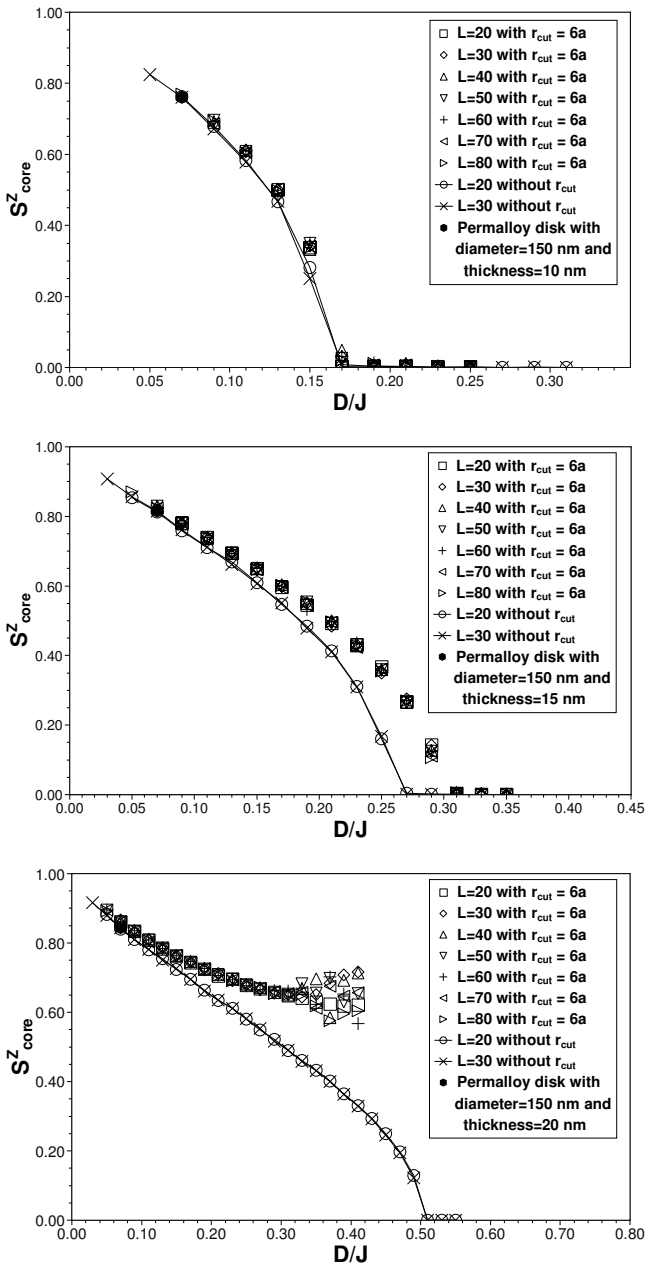


FIG. 3. Behavior of the out-of-plane component,  $S_{core}^z$ , as a function of the dipole interaction strength  $D$  (in units of  $J$ ). From top to bottom are shown the results for  $z=2, 3$ , and  $4$ , respectively. The diameters of the nanodisks are shown in the insets. In some results were used a cutoff  $r_{cut}=6a$  in the dipole interaction. The circles and diagonal crosses represent the results  $L=20$  and  $L=30$  for the dipole interaction with no cut-off. The black circles (●) represent the results for Permalloy-79 nanodisks with diameter 150 nm thickness 10 nm, 15 nm, and 20 nm, respectively. Error bars are smaller than the symbols when not visible. The lines are guides for the eyes.

suggested in Ref. 34. This finding is in agreement with experimental results.<sup>11</sup> In Fig. 3 we show the behavior of the out-of-plane component at the center of the vortex ( $S_{core}^z$ ) as a function of  $D/J$  for several diameters of the nanodisk. We observed a crossover between out-of-plane to in-plane configuration. A function of the type  $S_{core}^z \approx (D_c - D)^\alpha$  with  $\alpha \approx 0.55$ , describes very well the crossover line for each thickness considered. We also considered the application of an magnetic external field parallel to the plane of the disk to study the gyrotropic mode as a function of the out-of-plane

vortex-core magnetization. The results clearly show that there is a minimum value for the modulus of the  $S_{core}^z$  from which it is possible to excite the gyrotropic mode. This minimum value depends on the thickness of the nanodisk. In the next sections we show in detail the way our calculations were done. The paper is organized as follows: in Sec. II we describe the model and the numerical methods we used. In Sec. III we present and discuss our results. We also present in this section, theoretical results for Permalloy nanodisks obtained from our model. Section IV is dedicated to our conclusions.

## II. MODEL AND METHODOLOGY

The dipole interaction [the second term in Eq. (1)] is in general very difficult to treat in any analytical or computational approach due to its long range character. Much of the work done so far uses a variation of that Hamiltonian by considering an anisotropic interaction  $\Sigma(\vec{S} \cdot \vec{n})^2$  instead of the dipole term.<sup>35</sup> Here,  $\vec{n}$  represents a unit vector perpendicular to the surface and to the borderline of the system. This term contributes positively to the total energy, therefore, it forces the spins to be perpendicular to  $\vec{n}$ , competing with the exchange energy. The effect produced by this anisotropic interaction is similar to that one of the dipole term. The energy due to this term is minimized when the magnetic moments arrange themselves in a curling vortex structure. The low temperature properties of the Hamiltonian with the anisotropic term is similar to the one obtained by using the long range dipole interaction. Dealing with this alternative form saves a lot of cpu time in numerical approaches since it is not necessary to handle the sum over the entire lattice. However, the high temperature and the dynamical behaviors are quite different from the original model. As we want to explore the model beyond its low temperature properties, we treat the system by using Eq. (1). In many theoretical, as well as computational works done so far, a considerable simplification is to consider a 2D model. The results obtained by using this simplification are in reasonable qualitative agreement with experimental findings. Part of the present work is dedicated to discuss the influence of the thickness in the pure three-dimensional (3D) model. To define the nanodisk we proceed as follows. A number of magnetic particles is distributed over the sites of a cubic lattice. A disk of diameter  $d=La$  ( $L$  is an integer) centered in a previously chosen cell and thickness  $l=za$  is drawn over the array. The sites outside the disk are erased. The sites left inside form the nanodisk, that is the object of our interest. Here,  $a$  is the lattice parameter defined as the distance between first neighbors sites in lattice and  $z$  is an integer representing the number of layers considered in our 3D nanodisk model. As a matter of simplification from now on distances will be measured in units of  $a$  (we consider  $a=1$ ) and energy in units of  $J$  (we consider  $J=1$ ). Thus, in our simulations the nanodisk will be a small cylinder of diameter  $L$  and thickness  $z$ . Also, we consider the application of an external magnetic field  $\vec{h}_{ext}$  to study the behavior of the vortex gyrotropic mode. The magnetic field contributes to the hamiltonian with an additional term  $-\Sigma_i \vec{S}_i \cdot \vec{h}_{ext}$ . Due to the out-of-plane vortex-core magnetiza-

tion, under the influence of a weak in-plane magnetic field the vortex starts to move and its core behaves like a particle during the motion. The vortex acquires a gyration movement with a certain frequency that depends on the diameter of the nanodisk. The dynamics of the spins can be described by a discrete version of the Landau–Lifshitz (LL) equation:<sup>36,37</sup>

$$\frac{d\vec{S}_i}{dt} = - \left[ \vec{S}_i \times \frac{\partial H}{\partial \vec{S}_i} \right], \quad (2)$$

where  $S = |\vec{S}|$ . A detailed discussion about this formula can be found in Ref. 17. Alternatively the equations of motion can be obtained as

$$\dot{\Theta}_i = \frac{\partial H / \partial \Phi_i}{\cos \Theta_i}, \quad \dot{\Phi}_i = \frac{\partial H / \partial \Theta_i}{\cos \Theta_i}, \quad (3)$$

where  $\Theta$  and  $\Phi$  are spherical angles parameterizing the classical spin  $\vec{S}$

$$\vec{S}_i = (\cos \Theta_i \cos \Phi_i, \cos \Theta_i \sin \Phi_i, \sin \Theta_i). \quad (4)$$

Here  $\Phi_i$  and  $S_z = \sin \Theta_i$  constitute a pair of canonically conjugated variables.

### A. Ground state

In order to obtain the ground state configurations of the system we have used a simulated annealing approach.<sup>38</sup> Choosing an initial configuration of the spins as a planar vortex structure, the iterative simulated annealing process is implemented starting at temperature  $T_{init} = 0.1$  until the minimum  $T_{min} = 10^{-2}$ . Steps in temperature,  $\Delta T$ , were chosen so that the acceptance rate is maintained in 50%. Following, we introduced a dissipative term in the equations of motion which were solved employing a fourth-order predictor-corrector method. This cools down the system assuring that the nanodisk ground state is reached. To study the  $S_{core}^z$  behavior of the ground state as a function of  $D$  and of the system size we performed several numerical simulations following the methodology described above, so that, our results were obtained by performing an average over  $10^5$  different configurations. We varied the dipole strength  $D$  in the range 0.02–0.55, for several values of  $L$ , with  $20 \leq L \leq 80$ , and for  $z = 2, 3, 4$ . All configurations were saved to be used latterly as initial configurations in the study of the gyrotropic mode. In order to understand the effect of cutting off the range of the dipole energy term we worked the interaction with  $r_{cut} = 6a$  and without the cut-off ( $r_{cut} = L$ ).

### B. Dynamics

Once we have obtained the configurations at low temperature they are used as initial configurations to study the dynamics of the model. The dynamics of the system is followed by solving numerically the equations of motion using a fourth-order predictor-corrector scheme. If there is no external field applied the vortex remains at the center of the nanodisk. We introduced an in-plane external magnetic field so that a torc appears in the vortex obliging it to move in a direction perpendicular to the field. As soon as it start to

move a  $S_z$  component appears, as a consequence of the relationship between  $\Phi_i$  and  $S_z$ . By measuring the position of the center of the vortex as a function of the time we can describe its motion due to the presence of the magnetic field.

## III. RESULTS AND DISCUSSION

To investigate the formation of the vortex-core with out-of-plane magnetization we performed simulations varying the dipole strength  $D$  (in units of  $J$ ) in the range 0.02–0.55, for several diameter with  $20 \leq L \leq 80$ , and thickness with  $z = 2, 3, 4$ . In order to observe the influence of a cut-off,  $r_{cut}$ , the simulations were performed by considering  $r_{cut} = 6a$  and  $r_{cut} = La$  (no cut-off). From Fig. 3 we can see that as the thickness increases ( $z$  increases) the cutoff introduces stronger distortions in the behavior of  $S_{core}^z$ .

It is clear from Fig. 3 that there exists a crossover value ( $D = D_c$ ) separating the vortex regions with in-plane and the out-of-plane components. We observed that  $D_c$  is independent of the diameter  $L$  of the nanodisk but is strongly dependent on the thickness  $z$ . For  $z = 2, 3$ , and  $4$  we have obtained ( $D_c/J$ )  $\approx 0.165, 0.260$ , and  $0.510$ , respectively. The increasing of  $D_c$  with increasing  $z$  indicates that increasing the thickness has the same effect as introducing an anisotropy that causes a lowering in the necessary vortex energy to develop the out-of-plane component<sup>19–22</sup> which is in agreement with the results of Ref. 11. The behavior of  $S_{core}^z$  as a function of the dipole constant is well described by a function of the following type:

$$S_{core}^z \propto (D_c - D)^\alpha. \quad (5)$$

The exponent  $\alpha$  can be estimated by plotting  $\ln(S_{core}^z)$  as a function of  $\ln(D_c - D)$  for values of  $D$  near  $D_c$ . In Fig. 4 we show the plots where the results for the infinite range interaction (no cut-off) were used. The plots are for  $z = 2, 3$ , and  $4$  and the estimated  $\alpha$  are  $\alpha \approx 0.57, 0.57$ , and  $0.54$ , respectively. These results suggest that  $\alpha$  is independent of the thickness of the nanodisk.

To study the behavior of the gyrotropic mode, we consider the application of an in-plane external magnetic field  $\vec{h}_{ext}$  with  $|\vec{h}_{ext}| = 0.03J$ . This value ensures that the gyrotropic mode is excited without destroying the vortex state. In Fig. 5 we plot the vortex core  $x$  position (in units of lattice parameter  $a$ ) as function of time (in units of  $J$ ) for a nanodisk with  $L = 20$ ,  $z = 2$ , considering  $D = 0.10J$  ( $S_{core}^z = 0.61$ ) [Fig. 5(a)],  $D = 0.11J$  ( $S_{core}^z = 0.55$ ) [Fig. 5(b)],  $D = 0.12J$  ( $S_{core}^z = 0.50$ ) [Fig. 5(c)], and  $D = 0.13J$  ( $S_{core}^z = 0.45$ ) [Fig. 5(d)]. For  $z = 2$ , if  $S_{core}^z < 0.50$ , there is no gyrotropic mode. In Fig. 6 we plot the vortex core  $x$  position as function of time for a nanodisk with  $L = 20$ ,  $z = 3$ , considering  $D = 0.17J$  ( $S_{core}^z = 0.55$ ) [Fig. 6(a)],  $D = 0.19J$  ( $S_{core}^z = 0.50$ ) [Fig. 6(b)],  $D = 0.20J$  ( $S_{core}^z = 0.45$ ) [Fig. 6(c)], and  $D = 0.21J$  ( $S_{core}^z = 0.40$ ) [Fig. 6(d)]. For  $z = 3$ , we observe if  $S_{core}^z < 0.55$ , there is no gyrotropic mode. And, in Fig. 7 we plot the vortex core  $x$  position as function of time for a nanodisk with  $L = 20$ ,  $z = 4$ , considering  $D = 0.21J$  ( $S_{core}^z = 0.63$ ) [Fig. 7(a)],  $D = 0.23J$  ( $S_{core}^z = 0.60$ ) [Fig. 7(b)],  $D = 0.27J$  ( $S_{core}^z = 0.55$ ) [Fig. 7(c)], and  $D = 0.33J$

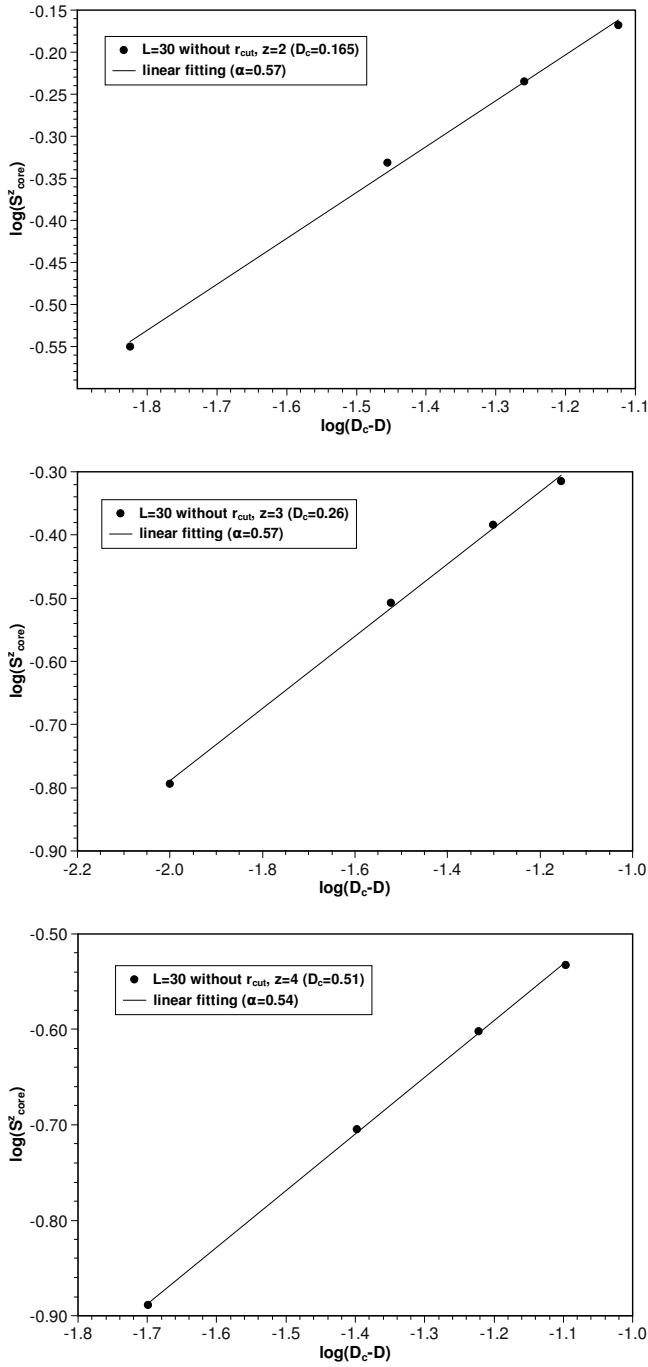


FIG. 4. Critical behavior of the  $\ln S_{core}^z$  as a function of  $\ln(D_c - D)$  for values of  $D$  close to  $D_c$ . From top to bottom are shown the results for  $z=2, 3$ , and  $4$ , respectively. In the figure are considered only the results with  $r_{cut}=L$  in the dipole interaction. The straight lines are linear adjusts with slope  $\alpha \approx 0.57, 0.57$ , and  $0.54$ , respectively.

( $S_{core}^z=0.46$ ) [Fig. 7(d)]. For  $z=4$ , we observe if  $S_{core}^z < 0.60$ , there is no gyrotropic mode.

The results clearly shown that there is a minimum value for the modulus of the  $S_{core}^z = S_{core-min}^z$  limiting the gyrotropic mode. We find for ( $z=2$ )  $S_{core-min}^z \approx 0.50$ , ( $z=3$ )  $S_{core-min}^z \approx 0.55$ , and for ( $z=4$ )  $S_{core-min}^z \approx 0.60$ . We observed that this minimum value increases with thickness. From these results we conclude that, if the thickness of the nanodisks increases, the vortex becomes more pinned.

We observe in Figs. 5–7 that, for fixed diameter, if the

thickness increases, the gyrotropic mode frequency increases. We conclude that the frequency increases with the aspect ratio,<sup>39</sup> which is in qualitative accordance with experimental findings.<sup>40,41</sup>

Using the micromagnetic approach<sup>42</sup> and known parameters we can produce results for real materials. In the micromagnetic approach the nanodisk is partitioned into cells containing many atoms. We consider the known parameters for Permalloy-79(Py) ( $Ni_{79}Fe_{21}$ ),<sup>43</sup> which are: exchange stiffness  $A=13 \text{ pJm}^{-1}$ , saturation magnetization  $M_s=860 \text{ K Am}^{-1}$ , and Curie temperature near  $630 \text{ K}$ . The Permalloy-79 has face-centered-cubic lattice structure with conventional unit cell parameter  $a_0=0.355 \text{ nm}$ . With these values we produce results for Permalloy nanodisks used in actual experiments. Following the methodology presented in Ref. 43 the system can be partitioned into cubical working cells of dimensions  $a \times a \times a$  and volume  $v_{cell}=a^3$ , where  $a$  is greater than unit cell parameter  $a_0$ . The spins in a working cell can be considered mostly aligned, hence the dipole moment in a cell has a fixed length  $\mu_{cell}$  equal to the saturation magnetization times the cell volume,  $\mu_{cell}=M_s v_{cell}$ . In our model of nanodisk each site  $i$  will now represent the center of a working cell. We consider in our micromagnetic simulations for Permalloy-79 nanodisks, the lattice parameter (distance center-to-center of neighboring working cells)  $a=5 \text{ nm}$ . This value is approximately the exchange length for the Permalloy-79 which is  $\lambda_{ex}=5.3 \text{ nm}$ . With this, the actual diameter  $d$  of the nanodisk is given by  $d=La$  and the actual thickness  $l$  by  $l=za$ . Considering a unit vector  $\hat{m}_i = \vec{\mu}_i / \mu_{cell}$  located in each site  $i$  [the vector  $\hat{m}_i$  is analogous to the vector  $\vec{S}_i$  that appears in (1)], where  $\vec{\mu}_i$  is the dipole moment of the working cell, the micromagnetic Hamiltonian for the system is given by<sup>43</sup>

$$H_{mic} = J_{cell} \left\{ - \sum_{\langle i,j \rangle} \hat{m}_i \cdot \hat{m}_j + \frac{D_{cell}}{J_{cell}} \sum_{i \neq j} \left[ \frac{\hat{m}_i \cdot \hat{m}_j}{(r_{ij}/a)^3} - \frac{3(\hat{m}_i \cdot \hat{r}_{ij}) \times (\hat{m}_j \cdot \hat{r}_{ij})}{(r_{ij}/a)^3} \right] \right\}. \quad (6)$$

Here  $J_{cell}$  is the effective exchange coupling between neighboring working cells,  $\hat{r}_{ij} = \vec{r}_{ij} / r_{ij}$  and  $D_{cell}$  is the effective strength of dipole–dipole interaction between working cells, given by

$$J_{cell} = 2Aa, \quad D_{cell} = \frac{\mu_0 \mu_{cell}^2}{4\pi a^3}. \quad (7)$$

The  $\mu_{cell}$  can be expressed as<sup>43</sup>

$$\mu_{cell} = 4 \left( \frac{a}{a_0} \right)^3 \mu_{atom}, \quad (8)$$

where  $\mu_{atom}$  is the magnitude of atomic magnetic dipole moment. The Permalloy has  $\mu_{atom}=9.62 \times 10^{-24} \text{ Am}^2$ , then using  $a=5 \text{ nm}$  and the parameters for Permalloy-79, we obtain  $\mu_{cell}=1.078 \times 10^{-19} \text{ Am}^2$ . From (7) we can estimate the ratio  $D/J$  for Permalloy-79(Py)

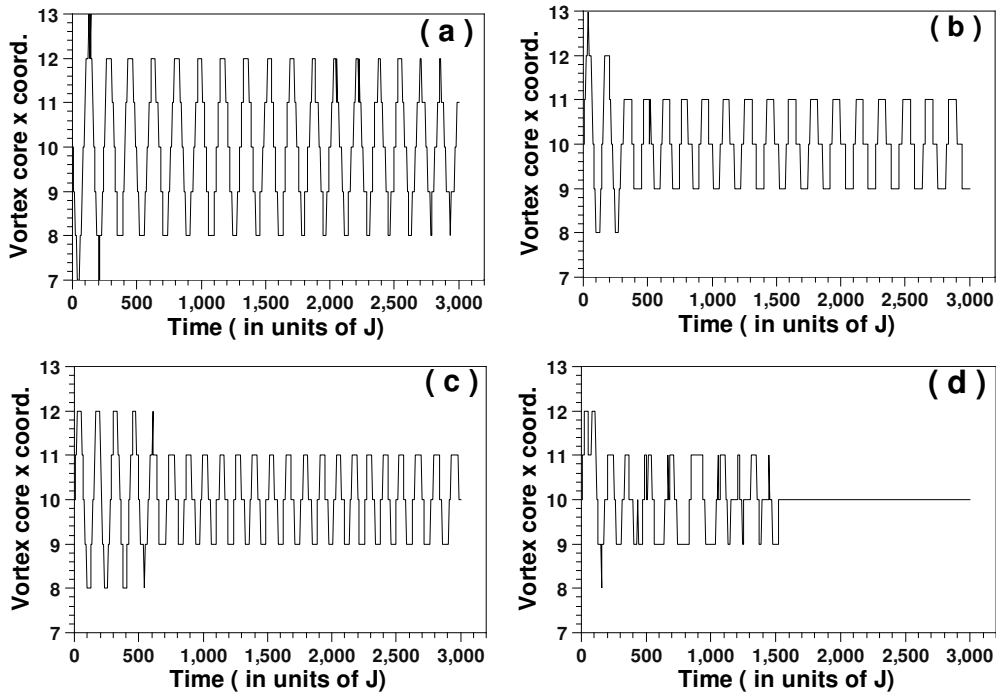


FIG. 5. Vortex core gyrotropic oscillation in nanodisks with thickness  $z=2$ . It is shown the vortex core  $x$  coordinate (in units of lattice parameter  $a$ ) vs time (in units of  $J$ ) for nanodisks with  $L=20$  (without  $r_{cut}$ ) and  $z=2$ . (a) shows the plot considering  $D=0.10J$  ( $S_{core}^z=0.61$ ). (b) shows the plot considering  $D=0.11J$  ( $S_{core}^z=0.55$ ). (c) shows the plot considering  $D=0.12J$  ( $S_{core}^z=0.50$ ). (d) shows the plot considering  $D=0.13J$  ( $S_{core}^z=0.45$ ).

$$\left(\frac{D}{J}\right)_{Py} = \frac{D_{cell}}{J_{cell}} = \frac{1}{4\pi} \left(\frac{a}{\lambda_{ex}}\right)^2 = 0.0708. \quad (9)$$

From Fig. 3 we can see that the ratio  $(D/J)_{Py} \ll (D_c/J)$  and Permalloy nanodisks with diameters  $d$  ( $d=La, a=5$  nm) in the range  $100 \text{ nm} \leq d \leq 400 \text{ nm}$  ( $20 \leq L \leq 80$ ) are in vortex state with an out-of-plane magnetization in its core ( $\mu_{core}^z$ ).

Also, we can observe from Fig. 3 that,  $\mu_{core}^z$  increases as the thickness  $l$  increases ( $l=za$ ; we consider  $z=2, 3$ , and 4, then  $l=10$  nm,  $l=15$  nm, and  $l=20$  nm, respectively). Both behaviors agree with experimental observations in Permalloy nanodisks.<sup>8,11</sup> The  $\mu_{core}^z$  is given by  $\mu_{core}^z = \mu_{cell} S_{core}^z$ .<sup>43</sup> Using  $S_{core}^z$  values taken from Fig. 3, we can estimate  $\mu_{core}^z$  to Per-

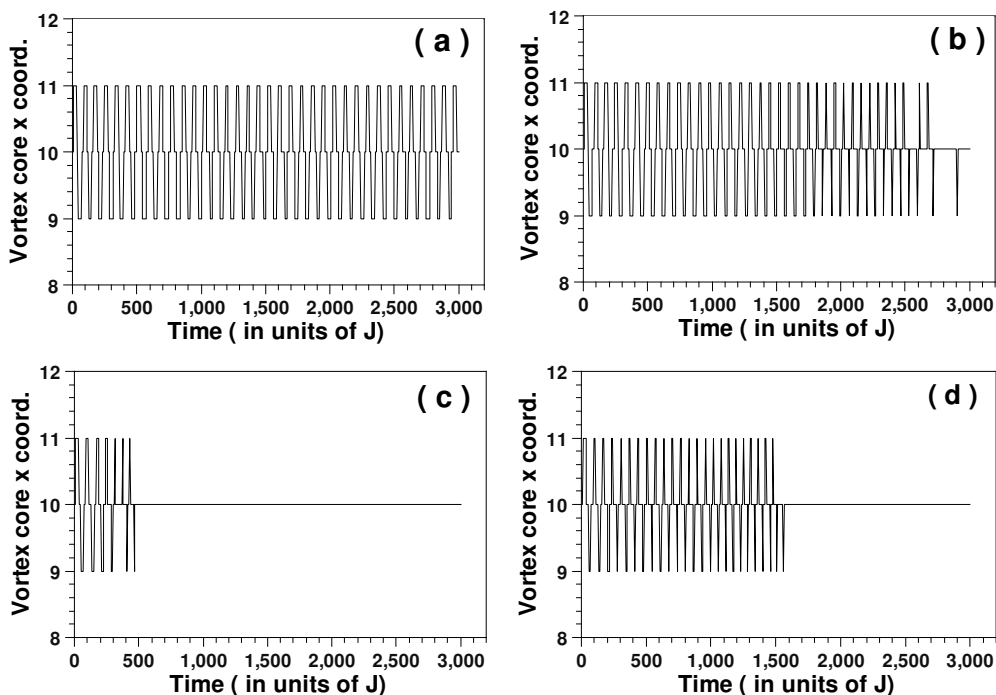


FIG. 6. Vortex core gyrotropic oscillation in nanodisks with thickness  $z=3$ . It is shown the vortex core  $x$  coordinate (in units of lattice parameter  $a$ ) vs time (in units of  $J$ ) for nanodisks with  $L=20$  (without  $r_{cut}$ ) and  $z=3$ . (a) shows the plot considering  $D=0.17J$  ( $S_{core}^z=0.55$ ). (b) shows the plot considering  $D=0.19J$  ( $S_{core}^z=0.50$ ). (c) shows the plot considering  $D=0.20J$  ( $S_{core}^z=0.45$ ). (d) shows the plot considering  $D=0.21J$  ( $S_{core}^z=0.40$ ).

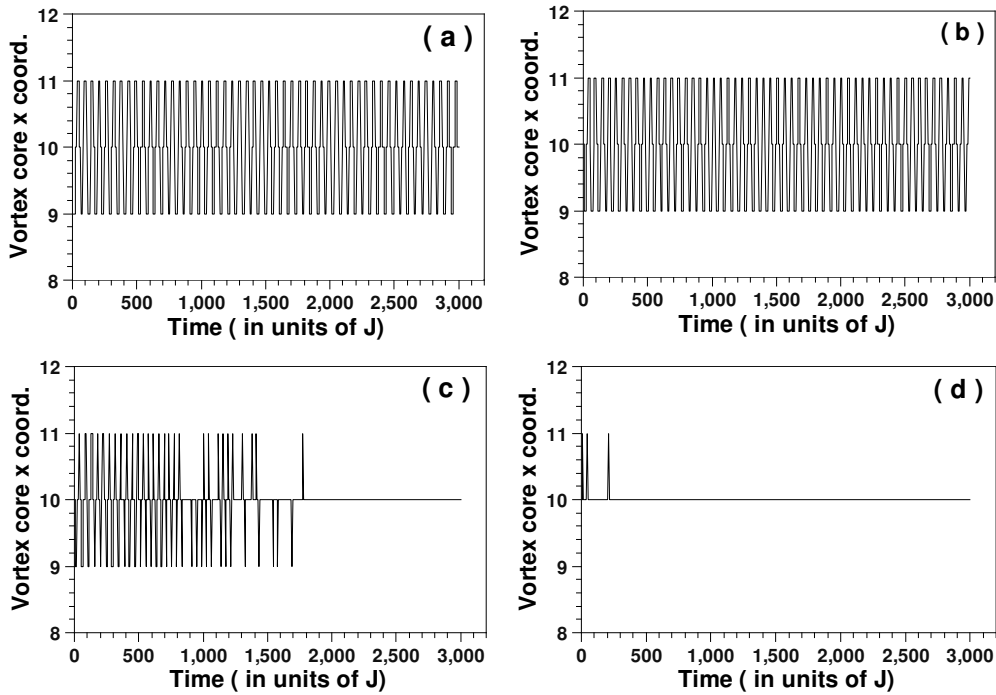


FIG. 7. Vortex core gyrotropic oscillation in nanodisks with thickness  $z=4$ . It is shown the vortex core  $x$  coordinate (in units of lattice parameter  $a$ ) vs time (in units of  $J$ ) for nanodisks with  $L=20$  (without  $r_{cut}$ ) and  $z=4$ . (a) shows the plot considering  $D=0.21J$  ( $S_{core}^z=0.63$ ). (b) shows the plot considering  $D=0.23J$  ( $S_{core}^z=0.61$ ). (c) shows the plot considering  $D=0.27J$  ( $S_{core}^z=0.55$ ). (d) shows the plot considering  $D=0.33J$  ( $S_{core}^z=0.46$ ).

malloy nanodisks. For nanodisks thickness 10 nm  $\mu_{core}^z \approx 8.2 \times 10^{-20}$  Am<sup>2</sup>, for thickness 15 nm  $\mu_{core}^z \approx 8.7 \times 10^{-20}$  Am<sup>2</sup> and for thickness 20 nm  $\mu_{core}^z \approx 9.1 \times 10^{-20}$  Am<sup>2</sup>.

To study the behavior of the gyrotropic mode in Permalloy-79 nanodisks we consider the application of an in-plane external magnetic field  $\vec{B}_{ap}$  of magnitude 10 mT. The magnetic field contributes to the micromagnetic Hamiltonian with an additional term  $-\mu_0 M_s^2 a^3 \sum_i \hat{m}_i \cdot \vec{h}_{ext}$ , where  $\vec{B}_{ap} = \mu_0 M_s \vec{h}_{ext}$ .<sup>43</sup> The time  $\tau$  (in seconds) is given by<sup>17</sup>

$$\tau = \frac{t}{\omega_0}, \quad (10)$$

where  $t$  is the simulation time (dimensionless) and  $\omega_0 = \mu_0 M_s \gamma$  ( $\gamma$  is a gyromagnetic ratio). For Permalloy-79,  $\omega_0 = 2.13 \times 10^{11}$  s<sup>-1</sup>.

Figures 8–10 show vortex core gyrotropic oscillations in Permalloy-79 nanodisks with a diameter  $d=175$  nm, thickness 10 nm, 15 nm, and 20 nm, respectively. We observed that the gyrotropic mode frequency lies in a sub gigahertz range (in megahertz range) and increases with the aspect ratio, which is in good accordance with experimental results for Permalloy nanodisks presented in Refs. 41 and 44.

#### IV. CONCLUSIONS

In this work we have used a numerical metropolis Monte Carlo method combined with spin dynamics simulations, to investigate the morphology of vortex-core in magnetic nanodisk. We have used a model Hamiltonian with exchange and dipolar interactions defined in a cubic lattice. The simulations were performed by considering the dipolar term with and without a cut-off. The results show clearly that the cut-

off in the dipolar interaction has to be taken very carefully. For  $z=2$  the results using a cut-off coincides with those without cut-off. However, for  $z=3,4$  we get completely unreliable results even for small values of  $D$ . Therefore, we have used the dipole interaction without any approximation. We observed that there is a critical value of dipole strength ( $D_c$ ) separating the in-plane vortex state from the out-of-plane vortex state which is independent of the diameter of nanodisk but depends on the thickness of the disk. The increasing of  $D_c$  with increasing  $z$  indicates that increasing the thickness has the same effect as introducing an anisotropy that causes a lowering in the necessary vortex energy to develop the out-of-plane component. The behavior of  $S_{core}^z$  as a function of the dipole constant is well described by a function ( $D_c$

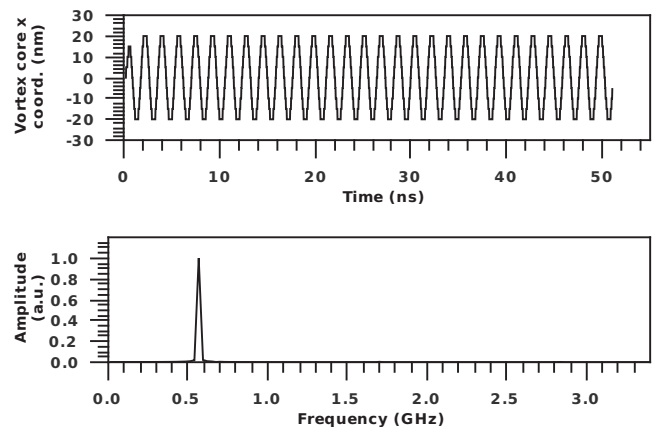


FIG. 8. Vortex core gyrotropic oscillation in Permalloy-79 nanodisk with diameter 175 nm and thickness 10 nm. At the top is shown the vortex core  $x$  coordinate (in nanometer) vs time (in nanosecond). At the bottom is shown its Fourier transform with amplitude in arbitrary units (atomic unit).



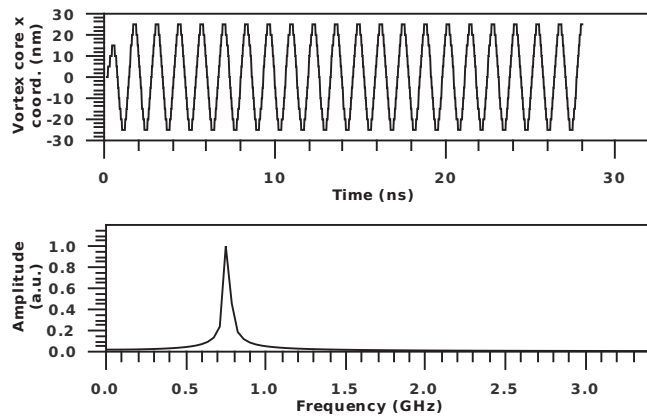


FIG. 9. Vortex core gyrotropic oscillation in Permalloy-79 nanodisk with diameter 175 nm and thickness 15 nm. At the top is shown the vortex core  $x$  coordinate (in nanometer) vs time (in nanosecond). At the bottom is shown its Fourier transform with amplitude in arbitrary units (atomic unit).

$-D)^\alpha$  with  $\alpha=0.55(2)$ , where  $\alpha$  seems to be a universal exponent independent of  $L$ ,  $D$ , and  $z$ . The application of an in-plane external magnetic field obliges the vortex to move in a direction perpendicular to the field. As soon as it starts to move a  $S_z$  component appears. This is an effect due to the relationship between  $\Phi_i$  and  $S_z$ . That is a mechanism already observed in the pure Heisenberg model in two dimensions.<sup>22</sup> By measuring the position of the center of the vortex as a function of the time we can describe its motion due to the presence of the magnetic field. We observe that there is a minimum value for the modulus of the  $S_{core}^z$ , from which we can excite the gyrotropic mode. This minimum value increases if the thickness of the nanodisk increases, which means that the vortex becomes more pinned. This result suggests that a way to improve the stability of the process of switching may be through the thickness control which is way technologically simple to do. We also observed that the gyrotropic mode frequency increases with the aspect ratio, which is in qualitative accordance with experimental results. Finally, using the micromagnetic approach and the known parameters, we estimated the ratio  $D/J$  for Permalloy-79. We observed that Permalloy nanodisks with diameters  $d$  in the range  $100 \text{ nm} \leq d \leq 400 \text{ nm}$  are in vortex

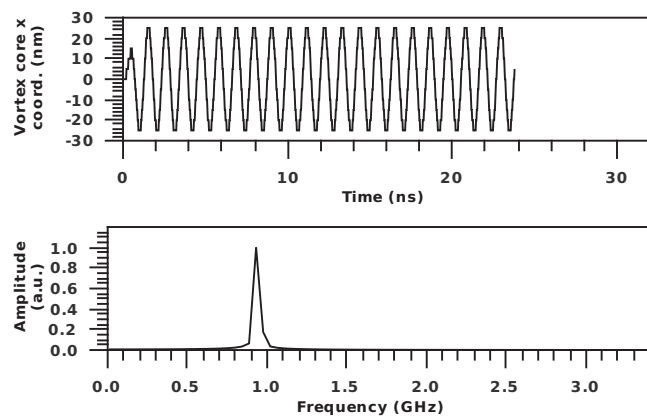


FIG. 10. Vortex core gyrotropic oscillation in Permalloy-79 nanodisk with diameter 175 nm and thickness 20 nm. At the top is shown the vortex core  $x$  coordinate (in nanometer) vs time (in nanosecond). At the bottom is shown its Fourier transform with amplitude in arbitrary units (atomic unit).

state with an out-of-plane magnetization in its core ( $\mu_{core}^z$ ) which increases as the thickness  $l$  increases. Also we observed gyrotropic oscillations in Permalloy-79 nanodisks with gyrotropic mode frequency in a sub GHz range, which increases with the aspect ratio. These behaviors agree with experimental observations in Permalloy nanodisks.

## ACKNOWLEDGMENTS

This work was partially supported by CNPq and FAPEMIG (Brazilian Agencies). Numerical works was done at the Laboratório de Simulação Computacional do Departamento de Física da UFJF.

- <sup>1</sup>K. Y. Guslienko, R. H. Heredero, and O. Chubykalo-Fesenko, *Phys. Rev. B* **82**, 014402 (2010).
- <sup>2</sup>J. Mejía-López, D. Altbir, P. Landeros, J. Escrig, A. H. Romero, I. V. Roshchin, C.-P. Li, M. R. Fitzsimmons, X. Batlle, and I. K. Schuller, *Phys. Rev. B* **81**, 184417 (2010).
- <sup>3</sup>S.-H. Chung, R. D. McMichael, D. T. Pierce, and J. Unguris, *Phys. Rev. B* **81**, 024410 (2010).
- <sup>4</sup>Y. Gaididei, V. P. Kravchuk, D. D. Sheka, and F. G. Mertens, *Phys. Rev. B* **81**, 094431 (2010).
- <sup>5</sup>D. Ruzmetov and V. Chandrasekhar, *J. Magn. Magn. Mater.* **320**, 47 (2008).
- <sup>6</sup>S.-H. Chung, D. T. Pierce, and J. Unguris, *J. Magn. Magn. Mater.* **110**, 177 (2010).
- <sup>7</sup>P. Candeloro, A. Gerardino, E. Di Fabrizio, S. Cabrini, G. Giannini, L. Mastrogiacomo, M. Ciria, R. C. O'Handley, G. Gubbiotti, and G. Carlotti, *Jpn. J. Appl. Phys., Part 1* **41**, 5149 (2002).
- <sup>8</sup>R. P. Cowburn, D. K. Koltsov, A. O. Adeyeye, M. E. Welland, and D. M. Tricker, *Phys. Rev. Lett.* **83**, 1042 (1999).
- <sup>9</sup>C. A. Ross, *Annu. Rev. Mater. Res.* **31**, 203 (2001).
- <sup>10</sup>C. A. Ross, M. Hwang, M. Shima, J. Y. Cheng, M. Farhoud, T. A. Savas, H. I. Smith, W. Schwarzacher, F. M. Ross, M. Redjail, and F. B. Humphrey, *Phys. Rev. B* **65**, 144417 (2002).
- <sup>11</sup>T. Shinjo, T. Okuno, R. Hassdorf, K. Shigeto, and T. Ono, *Science* **289**, 930 (2000).
- <sup>12</sup>S. Chikazumi, *Physics of Ferromagnetism* (Oxford University Press, New York, 1997).
- <sup>13</sup>V. L. Berezinskii, *Sov. Phys. JETP* **32**, 493 (1971).
- <sup>14</sup>J. M. Kosterlitz and D. J. Thouless, *J. Phys. C* **6**, 1181 (1973).
- <sup>15</sup>V. E. Kireev and B. A. Ivanov, *Phys. Rev. B* **68**, 104428 (2003).
- <sup>16</sup>S. A. Leonel, I. A. Marques, P. Z. Coura, and B. V. Costa, *J. Appl. Phys.* **102**, 104311 (2007).
- <sup>17</sup>L. Berger, Y. Labaye, M. Tamine, and J. M. D. Coey, *Phys. Rev. B* **77**, 104431 (2008).
- <sup>18</sup>See, for example, A. Hubert and R. Schafer, *Magnetic Domains* (Springer, Berlin 1998).
- <sup>19</sup>S. Hikami and T. Tsuneto, *Prog. Theor. Phys.* **63**, 387 (1980).
- <sup>20</sup>S. Takeno and S. Homma, *Prog. Theor. Phys.* **64**, 1193 (1980).
- <sup>21</sup>G. M. Wysin, *Phys. Rev. B* **49**, 8780 (1994).
- <sup>22</sup>J. E. R. Costa and B. V. Costa, *Phys. Rev. B* **54**, 994 (1996); J. E. R. Costa, B. V. Costa, and D. P. Landau, *ibid.* **57**, 11510 (1998).
- <sup>23</sup>R. P. Cowburn, *Nature Mater.* **6**, 255 (2007).
- <sup>24</sup>A. A. Thiele, *Phys. Rev. Lett.* **30**, 230 (1973).
- <sup>25</sup>D. L. Huber, *Phys. Rev. B* **26**, 3758 (1982).
- <sup>26</sup>S. B. Choe, Y. Acremann, A. Scholl, A. Bauer, A. Doran, J. Stohr, and H. A. Padmore, *Science* **304**, 420 (2004).
- <sup>27</sup>H. Stoll, A. Puzic, B. Van Waeyenberge, P. Fischer, J. Raabe, M. Buess, T. Haug, R. Hollinger, C. Back, D. Weiss, and G. Denbeaux, *Appl. Phys. Lett.* **84**, 3328 (2004).
- <sup>28</sup>B. Van Waeyenberge, A. Puzic, H. Stoll, K. W. Chou, T. Tylliszczak, R. Hertel, M. Fähnle, H. Brückl, K. Rott, G. Reiss, I. Neudecker, D. Weiss, C. H. Back, and G. Schütz, *Nature (London)* **444**, 461 (2006).
- <sup>29</sup>J. P. Park, P. Eames, D. M. Engebretson, J. Berezovsky, and P. A. Crowell, *Phys. Rev. B* **67**, 020403 (2003).
- <sup>30</sup>J. Raabe, C. Quitmann, C. H. Back, F. Nolting, S. Johnson, and C. Buehler, *Phys. Rev. Lett.* **94**, 217204 (2005).
- <sup>31</sup>Y. Gaididei, V. P. Kravchuk, and D. D. Sheka, *Int. J. Quantum Chem.* **110**, 83 (2010).

- <sup>32</sup>For a revision on the subject see: S. Prakash, *Phys. Rev. B* **42**, 6574 (1990); A. B. MacIsaac, J. P. Whitehead, K. DeBell, and P. H. Poole, *Phys. Rev. Lett.* **77**, 739 (1996); A. Hucht and K. D. Usadel, *J. Magn. Magn. Mater.* **156**, 423 (1996); A. B. MacIsaac, K. DeBell, and J. P. Whitehead, *Phys. Rev. Lett.* **80**, 616 (1998); E. Y. Vedmedenko A. Ghazali, and J.-C. S. Lévy, *Phys. Rev. B* **59**, 3329 (1999); E. Y. Vedmedenko, H. P. Oepen, A. Ghazali, J.-C. S. Lévy, and J. Kirschner, *Phys. Rev. Lett.* **84**, 5884 (2000); E. Birsan, *J. Supercond. Novel Magn.* **22**, 711 (2009).
- <sup>33</sup>A. Vansteenkiste, K. W. Chou, M. Weigand, M. Curcic, V. Sackmann, H. Stoll, T. Tylliszczak, G. Woltersdorf, C. H. Back, G. Schütz, and B. Van Waeyenberg, *Nat. Phys.* **5**, 332 (2009).
- <sup>34</sup>J. C. S. Rocha, P. Z. Coura, S. A. Leonel, R. A. Dias, and B. V. Costa, *J. Appl. Phys.* **107**, 053903 (2010).
- <sup>35</sup>C. Zhou, T. C. Schulthess, and D. P. Landau, *J. Appl. Phys.* **99**, 08H906 (2006); R. H. Kodama, A. E. Berkowitz, E. J. McNiff, Jr., and S. Foner, *Phys. Rev. Lett.* **77**, 394 (1996); V. P. Shilov, Y. L. Raikher, J. C. Bacri, F. Gazeau, and R. Perzynski, *Phys. Rev. B* **60**, 11902 (1999); A. Aharoni, *J. Appl. Phys.* **61**, 3302 (1987); **69**, 7762 (1991); **81**, 830 (1997); **87**, 5526 (2000).
- <sup>36</sup>L. D. Landau and E. M. Lifshitz, *Phys. Z. Sowjetunion* **8**, 153 (1935); L. D. Landau, in *Collected Papers*, edited by D. ter Haar (Gordon and Breach, New York, 1967), p. 101.
- <sup>37</sup>T. L. Gilbert, *IEEE Trans. Magn.* **40**, 3443 (2004).
- <sup>38</sup>V. B. Nascimento, V. E. de Carvalho, C. M. C. de Castilho, B. V. Costa, and E. A. Soares, *Surf. Sci.* **487**, 15 (2001).
- <sup>39</sup>K. Y. Guslienko, B. A. Ivanov, V. Novosad, V. Y. Otani, H. Shima, and K. Fukamichi, *J. Appl. Phys.* **91**, 8037 (2002).
- <sup>40</sup>V. Novosad, F. Y. Fradin, P. E. Roy, K. S. Buchanan, K. Y. Guslienko, and S. D. Bader, *Phys. Rev. B* **72**, 024455 (2005).
- <sup>41</sup>K. Y. Guslienko, X. F. Han, D. J. Keavney, R. Divan, and S. D. Bader, *Phys. Rev. Lett.* **96**, 067205 (2006).
- <sup>42</sup>D. Suessa, J. Fidler, and T. Schrefl, *Handbook of Magnetic Materials* (Elsevier, Amsterdam, 2006), Vol. 16, p. 41.
- <sup>43</sup>G. M. Wysin, *J. Phys.: Condens. Matter* **22**, 376002 (2010).
- <sup>44</sup>C. E. Zaspel, B. A. Ivanov, J. P. Park, and P. A. Crowell, *Phys. Rev. B* **72**, 024427 (2005).